Published in final edited form as:

Neurobiol Dis. 2015 October ; 82: 123–131. doi:10.1016/j.nbd.2015.06.001.

Development-Dependent Regulation of Molecular Chaperones after Hypoxia-Ischemia

Xin Sun[1,2], **Robert Crawford**[1], **Chunli Liu**[1], **Tianfei Luo**[1], and **Bingren Hu**[1,*]

[1]Shock Trauma and Anesthesiology Research Center, University of Maryland School of Medicine, USA

[2]Department of Neurology, The First Teaching Hospital, Jilin University, China

Abstract

Cellular stress response after hypoxia-Ischemia (HI) may be substantially different between immature and mature brain. To study this phenomenon, postnatal day 7 (P7) and P26 rats were subjected to HI followed by different periods of recovery. Nuclear accumulation of heat-shock transcription factor-1 (HSF1) and expression of molecular chaperone proteins and mRNAs were analyzed by in situ hybridization, Western blotting and confocal microscopy. Nuclear accumulation of HSF1 protein and induction of hsp70 mRNA occurred dramatically in P26 neurons, but minimally in P7 neurons and moderately in microglial cells after HI. Consistently, the level of HSF1 was significantly higher in P26 brain samples, compared with that in P7 brain. Translation of hsp70 mRNA into proteins in P26 mature neurons were seen at 4 h and peaked at 24 h, when some neurons had already died after HI. Induction of ER glucose-regulated protein-78 (grp78) and mitochondrial hsp60 mRNAs and proteins was moderate and occurred also only in P26 mature brain after HI. These results suggest that the cellular stress response after HI is development-dependent, being pronounced in mature but virtually negligible in neonatal neurons. Therefore, the effectiveness of therapeutic strategies targeting the stress pathway against HI may be significantly different between immature and mature brains. The delayed induction of molecular chaperones in mature brain may be somewhat late for protecting HI neurons from acute HI injury.

Keywords

hypoxia-ischemia; brain development; neonatal; neuronal death; molecular chaperones; protein aggregation; ER stress

*Correspondence: Bingren Hu, MD, PhD., bhu@anes.umm.edu.

Disclosures: None

Introduction

A single episode of brain HI is able to induce neuronal death and long-term neurological deficits. It has long been known that neuronal death mechanisms for neonatal and mature neurons after HI are significantly different (Hu et al., 2000; Tang et al., 2004; Liu et al., 2004; Wang et al., 2009; Zhu et al., 2009). For example, neonatal neurons have dominant built-in apoptotic machinery that gradually fades out during brain maturation (Hu et al., 2000; Liu et al., 2004; Blomgren et al., 2007). Molecular chaperones play a major role in preventing toxic protein aggregation by shielding hydrophobic segments of toxic unfolded proteins. Under physiological conditions, the levels of constitutive molecular chaperones are sufficient to protect the normal levels of newly synthesized unfolded proteins during their folding and assembly (Hartl and Hayer-Hartl, 2002). Under ischemic conditions, however, the ATP-dependent molecular chaperone processing capacity is significantly reduced, resulting in toxic protein aggregation in mature neurons (Hu et al., 2000 and 2001; Liu et al., 2005a; Zhang et al., 2006). Despite the recent progress, how HI regulates expression of molecular chaperones differentially between neonatal and mature brains remains unknown.

Cells cope with stress, such as hyperthermia or ischemia, by expressing inducible molecular chaperones such as heat shock proteins (HSPs) to prevent toxic protein misfolding or aggregation, the so-called heat shock response (HSR) (Truettner et al., 2009). HSR is initiated at the transcription level by heat-shock transcription factors (HSFs). In vertebrates, four HSF family members (HSF1, HSF2, HSF3, and HSF4) have been identified. HSF1 is the master regulator of HSR in mature neurons (Fujimoto and Nakai, 2010). Activation of HSF1 leads to its nuclear translocation and induction of more than 3000 genes; including the classical molecular chaperone genes such as HSP70, Hdj1, Hdj4, Hdj6, HSP27 and HSP25, as well as the non-classical heat shock genes (Song et al., 2010; Islam et al., 2013). For that reason, drug-induced activation of HSR has been used as an experimental strategy to show that induction of HSR offers strong cell protection in cellular, worm, fly, and mouse or rat models (e.g., Lu et al., 2002; Harrison et al., 2008; Batulan et al., 2006; Neef et al., 2010; Liu et al., 2011; Verma et al., 2014; Ambade et al., 2014; Cha et al., 2014). However, activation of HSF1 may also have undesired effects. For instance, HSF1 activation may facilitate the survival of cancer cells (Vydra et al., 2013). This study shows that HSR after HI is dramatically different between immature and mature neurons. Therefore, the effectiveness of therapeutic strategies targeting HSR against HI may also be different between immature and mature brains.

Materials and Methods

Materials

Leupeptin, pepstain, aprotinin, phenylmethylsulfonyl fluoride (PMSF), dithiothreitol (DTT), Triton X-100 (TX100), sodium dodecyl sulfate (SDS), propidium iodide and other chemicals, as well as antibodies to beta-actin, Iba-1, and GFAP were purchased from Sigma (St. Louis, MO). Antibodies to Hsp40, Hsp70, Hsp90, Grp78, Grp94, calnexin, and PDI were purchased from Stressgen Biotechnologies, Inc. (San Diego, CA). Active caspase 3 and HSF1 antibodies were purchased from Cell Signaling Tech (Danvers, MA). Secondary antibodies were purchased from Jackson ImmunoResearch Labs (West Grove, PA).

Hypoxia/ischemia animal model

Animal studies were conducted in accordance with the Guide for the Care and Use of Laboratory Animals published by the National Institutes of Health and were approved by the animal care committee of the University of Maryland. Pregnant Sprague-Dawley rats were purchased from Charles River Laboratories (Wilmington, MA) and housed in individual cages. The newborn rat pups were housed with their dams until weaning at postnatal day 21. Brain hypoxia-ischemia (HI) was induced by a combination of ligation of the left common carotid artery (CCA) and systemic hypoxia (8% O2) (Rice et al., 1981). The birth date is designated as postnatal day 1 (P1). Rats at P7 and P26 days were anesthetized with isoflurane (4% induction and 1% maintenance). A midline neck incision was made; thereafter, the left CCA was exposed and ligated permanently. The incision was sutured and the rats were returned to their dams or original cages. Following 1 h of recovery, the rats were placed in a hypoxic chamber through which humidified 8% oxygen with the balance nitrogen flowed for 60 min for the P7 rats, and for 30 min for the P26 rats. The concentration of oxygen flowing through the hypoxic system was monitored with an Ohmeda 5120 Oxygen Monitor (Madison, WI) during the entire experiment. The hypoxic duration in different groups of rats was chosen based on many published studies including our own, which show that the chosen intervals produce a similar severity of brain damage in P7 and P26 age groups (Blumenfeld et al., 1992; Towfighi and Mauger, 1997 and 1998; Hu et al., 2000b; Liu et al., 2004). The hypoxic chambers were partially submerged in a 37°C water bath to maintain normothermia during the HI periods. Under these conditions, rat body temperature during HI was 37.0 ± 0.15 (n = 7). After induction of HI, the animals were kept in the open chamber for about 30 min until they showed signs of recovery. They were then returned to their dams or cages. The hypoxia only controls were subjected to the same procedures but without ligation of the CCA. Brains were collected at 0.5, 4 and 24 h after HI.

In situ hybridization

Brains for in situ hybridization experiments were washed twice with RNase free phosphate-buffered saline (PBS), and put into small plastic containers filled with Tissue Tek OTC compound (Sakura Fine Technical Co., Tokyo, Japan). The brain samples were frozen in 2-methylbutane liquid at −40 °C and stored at −80 °C. Two levels (bregma 0.20 and −3.30) were cryosectioned at 12 μm onto Probe-on Plus slides (Fisher Scientific, Pittsburgh, PA), and stored at −80 °C until use. For later use, fresh frozen sections were thawed to room temperature and fixed for 5 min in 4% formaldehyde/phosphate-buffered saline. Sections were acetylated for 10 min at room temperature in 0.25% acetic anhydride and 0.1 M triethanolamine–HCl (pH 8), then dehydrated through a series of graded ethanol solutions, delipidized in 100% chloroform for 5 min, rinsed in 100% ethanol, and allowed to air dry.

Sections were hybridized to ^{35}S labeled riboprobes generated by in vitro transcription of the anti-sense strands of cDNA clones subcloned into transcription vectors using the Promega Riboprobe™ System. The plasmid containing a 248 bp Apa1–Xho1 fragment from the 3′ end of the rat HSP70 was provided by Dr. J. Truettner (the Miami Project, University of Miami Miller School of Medicine). The hamster Grp78 cDNA clone was provided by Dr.

Amy S. Lee (USC/Norris Cancer Center). The HSP60 cDNA clone was generously provided by Dr. Koichi Kokame (National Cardiovascular Center Research Institute, Osaka, Japan).

Hybridization with riboprobes was conducted as follows: the denatured probe (2×107 dpm/ml) was added to a solution containing 100 μg/ml salmon sperm DNA (ssDNA), 250 μg/ml each of yeast total RNA and tRNA, 50% formamide, 20 mM Tris–HCl (7.4), 1 mM EDTA, 300 mM NaCl, 10% dextran sulfate, and 1×Denhardts. The hybridization solution was added to the sections, covered with coverslips, and hybridized under humid conditions at 55 °C for 20 h. After removal of the coverslips, sections were washed at room temperature in a series of decreasing amounts of standard saline citrate (SSC) with 1 mM dithiothreitol (DTT) to a final concentration of 0.1×SSC. The slides were treated with 20 μg/ml RNAse A for 30 min at 37 °C. The final high-stringency wash was carried out in 0.1×SSC, 1 mM DTT for 1 h at 65 °C. Sections were dehydrated through a series of ethanols containing 300 mM ammonium acetate, ending with 100% ethanol. Sections were exposed to Kodak BIOMAX MR film at 4°C for various lengths of time. Negative control (sense strand) probes showed no hybridization signals (data not shown). Autoradiographs were digitized by a charge-coupled device camera (Xillix Technologies Corp., Canada) with a Micro Nikon 55 mm lens, which was interfaced to an image-analysis system (MCID Model M2, Imaging Research, Inc., Canada) and captured at 50 μm resolution. Optical density values in the entire ipsilateral or contralateral brain region at both the striatal and hippocampal levels (see Fig. 1A, left panels) were measured for each probe.

Confocal microscopy and histology

The rats were perfused with ice-cold 4% phosphate-buffered paraformaldehyde for confocal microscopy. Brains were cut with a Leica vibratome (Solms, Germany) at a thickness of 50 μm coronal brain sections (Hu et al., 2000a; Tang et al., 2004). Sections from sham-operated control rats and rats subjected to HI followed by 0.5, 4, and 24 h of recovery for both age groups were analyzed. Brain sections were washed with phosphate-buffered saline (PBS) containing 0.1% Triton X100 (TX100) for 30 min. Non-specific binding sites were blocked in 3% BSA in PBS/0.1% TX100 for 30 min. Primary antibodies were diluted 1:250 in PBS/0.1% TX100 and 1% BSA. After incubation overnight at 4°C, sections were washed in PBS containing 0.1% TX100, and were then incubated for 1 h at room temperature with either fluorescein-labeled anti-rabbit or lissamine rhodamine-labeled anti-mouse diluted 1:200, or propidium iodide (PI) (1 μg/ml) in PBS containing 1% BSA. Sections were washed several times in PBS and mounted on glass slides. Slides were analyzed on a Zeiss laser-scanning confocal microscope. For histology, 50 μm vibratome brain sections at two levels (bregma 0.20 mm and −3.6 mm) were mounted on glass slides, stained with hematoxylin and eosin, and then examined with a light microscope.

Subcellular fractionation

Tissue homogenates and subcellular fractions for Western blot analyses were prepared according to the method described previously (Tang et al., 2004). Brain tissue samples were obtained by freezing the brain in situ with liquid nitrogen (Ponten et al., 1973). Subcellular fractions were prepared from sham-operated, and post-HI rat brain tissues. The cortical brain tissues between bregma 1.70 mm and −4.52 mm of P7 and P26 rats were collected and

divided into ipsilateral and contralateral sides. Preparation of subcellular fractions was carried out either on ice or at 4°C. Brain tissue was cut into small pieces and homogenized with a Dounce homogenizer (25 strokes) in 10 vol. of ice-cold homogenization buffer containing 15 mM Tris base/HCl pH 7.6, 1 mM DTT, 0.25 M sucrose, 1 mM MgCl2, 1 μg/ml pepstain A, 5 μg/ml leupeptin, 2.5 μg/ml aproptonin, 0.5 mM PMSF, 2.5 mM EDTA, 1 mM EGTA, 0.25 M Na_3VO_4, 25 mM NaF and 2 mM sodium pyrophosphate. The homogenate was centrifuged at 800 g for 10 min to get the crude nuclear pellet (P1). The supernatant was then centrifuged at 10,000 g, for 10 min to obtain a crude pellet (P2) enriched with synaptosomes and mitochondria, and the resulting supernatant was further centrifuged at 165,000 g, for 1 h to get a cytosolic fraction (S3) and a microsomal fraction (P3) that contained intracellular membranes. Tissue homogenates and P1 and S3 fractions were used in this study. The contents of these subcellular fractions were verified in previous studies, demonstrating that P1 is a crude nuclear fraction, and S3 is a cytosolic fraction (Hu et al., 1998). Protein concentration was determined by a micro-bicinchoninic acid (BCA) method.

Western blot analysis

Equal protein amounts in subcellular fractions were electrophoresed on 10% sodium dodecyl sulfate-polyacrylamide gels (SDS-PAGE) and then transferred to Immobilon-P membranes (Millipore, Billerica, MA, USA). The membranes were incubated with 3% BSA in TBS for 30 min, and then overnight at 4ºC with a primary antibody. After washing, the membranes were further incubated with horseradish peroxidase-conjugated anti-rabbit or anti-mouse secondary antibodies for 1 h at room temperature. The β-actin levels on the immunoblots were also labeled as endogenous protein loading controls. The immunoblots were developed using enhanced chemiluminescence (ECL, Pierce Biosciences, Rockford, IL USA) and developed on Kodak X-omat LS film (Eastman Kodak Company, New Haven, CT, USA). Densitometry was performed with Kodak ID image analyses software (Eastman Kodak Company). All Western blot data were expressed as the ratio of the levels of the protein of interest and β-actin.

Statistical Analysis

One-way ANOVA followed by Tukey’s post hoc test was used for statistical analysis. Unpaired t-test was used for statistical analysis between P7 and P26 samples.

RESULTS

Induction of molecular chaperones after HI

The developmental stage of P7 rat brain in terms of cortical organization, synapse number and electrophysiological parameters, is similar to that of a 32- to 34-week gestation of human fetus or newborn infant (Romijn et al., 1991). Based on the levels of neuronal marker proteins (e.g., glutamate receptors and calcium/calmodulin-dependent kinase II) in brain tissue, previous studies show that rat brain is mostly matured during P21–P26 days (Martin et al., 1998; Tang et al., 2004). In situ hybridization and Western blotting were used to determine molecular chaperone mRNA and protein levels in P7 and P26 rat brains after HI. Induction of hsp70 mRNA was seen in the ipsilateral hemisphere throughout the cortical,

striatal, hippocampal and subcortical areas, and occurred as early as 0.5 h, peaked at 4 h, and remained elevated at 24 h of recovery at both the striatal (Fig. 1A, left, P7 and P26, Str) and hippocampal (Fig. 1A, left, P7 and P26, Hip) levels after HI. This occurred mainly in the ipsilateral hemispheres of P26 rat brains (Fig. 1A, left panels, P26, arrowhead). Hsp70 mRNA was also induced at 0.5, 4, and 24 h of recovery in the P26 hippocampal CA1 region of the contralateral hemisphere (Fig. 1A, left panels, P26, arrow), which was virtually identical to the hsp70 mRNA expression pattern of the hypoxia only controls (Supplement Fig. 1s, P26, Hypoxia alone). The induction of HSP70 mRNAs and proteins was very responsive to HI, as all sets of P26 HI brains had consistent and significant induction of molecular chaperones after HI (Supplement Fig. 1s). Compared with P26 brain regions, induction of hsp70 mRNA in P7 brains was particularly weak in the ipsilateral and was not detectable in the contralateral brains after HI (Fig. 1A, left panels, P7). Quantitative analysis confirmed that the quantity of hsp70 mRNA expression was increased dramatically in both the striatal level hemisphere (Fig. 1A, right panels, upper, Str-level Hemi) and the hippocampal level hemisphere (Fig. 1A, right panels, lower, Hip-level Hemi) of the P26, but to a significantly lesser degree in the P7 brain sections after HI.

To study HSP70 protein expression after HI, the ipsilateral hemispheres with HSP70 mRNA expression at both the striatal (Str) and hippocampal (Hip) levels were dissected out and combined (Fig. 1A, 30m, the drawing areas). The HSP70 protein level in the tissue lysates was analyzed with Western blotting (Fig. 1B). Consistent with HSP70 mRNA expression, HSP70 protein was consistently induced after HI dramatically in P26 brain samples, but only slightly in P7 brain samples (Fig. 1B). Relative to hsp70 mRNA, induction of HSP70 protein occurred in a delayed fashion, i.e., it was induced only moderately at 4 h, but dramatically at 24 h after HI (Fig. 1B). The beta-actin levels were unchanged between the sham-operated control samples and post-HI samples (Fig. 1B, P7 and P26, actin).

HSP60 is predominantly located in the mitochondrial matrix. Hsp60 mRNA was induced significantly in P26, but the induction was negligible in P7 brain sections after HI (Fig. 2A, left panels, arrow). Quantitative analysis revealed that hsp60 mRNA level was significantly increased mainly in P26 brain regions at both the striatal (Str) and hippocampal (Hip) levels after HI (Fig. 2A, right panels). However, the induction of HSP60 protein did not reach to the statistically significance during the measured recovery time points after HI (Fig. 2B). Moreover, the degree of hsp60 mRNA induction was markedly less than that of HSP70 mRNA after HI (compare Fig. 2A with Fig. 1A).

Similarly, the ER grp78 mRNA was also induced moderately, but significantly in P26 and minimally in P7 brain regions at 4 or 24 h of recovery after HI (Fig. 3A, arrowhead), while the level of GRP78 protein was not significantly changed in both P7 and P26 brain samples after HI (Fig. 3B).

Nuclear translocation of HSF1 and cellular expression of HSP70 protein after HI

The HSF1 protein redistribution between nuclear and cytosolic fractions was further studied in both P7 and P26 brain samples after HI (Fig. 4). Western blotting revealed that HSF1 was redistributed from the cytosolic S3 fraction (Fig. 4A) to the nuclear P1 fraction (Fig. 4B)

during 0.5, 4 and 24 h recovery periods, which occurred markedly in P26, but minimally in P7 brain samples after HI (Fig. 4, A and B).

We next performed double staining confocal microscopy of brain sections with HSF1 (red color) and HSP70 antibodies (green color) (Fig. 5). Paraformaldehyde-fixed brain sections were prepared from a different set of rats subjected to HI followed by different periods of recovery (Fig. 5). HSP70 mRNA was highly induced in the HI-affected neocortical and hippocampal CA1 and DG brain regions (see Fig. 1A), and some neurons in these brain regions were damaged at 48 h after HI (Supplement Fig. 2s) (Hu et al., 2000b; Liu et al., 2004). Fig. 5A shows that the level of the P26 HSF1 protein immunoreactivity was increased in the nuclei of the CA1, DG and neocortical regions slightly at 30 min, and reaching a plateau during 4 – 24 h after HI (Fig. 5A, arrows). Correspondingly, Fig. 5B shows that the level of the P26 HSP70 protein immunolabeling was upregulated, but in a relatively delayed fashion in the cytoplasm of the CA1, DG and neocortical regions, e.g., slightly at 4 h and markedly at 24 h after HI. In comparison with those in P26 brain sections, the level and pattern of the HSF1 protein immunoreactivities in P7 brain sections were not altered in the CA1, DG and neocortical (Cx) regions after HI (Fig. 5C, arrows). Consistently, in P7 brain sections, HSP70 protein was also not significantly induced in neurons.

We noticed that the pattern of the HSP70 protein immunostaining in 4 and 24 h reperfused P7 brain sections was suggestive of microglial expression (Fig. 5D, CA1 and Cx, double arrows). To study the possible microglial expression of HSP70, the following multi-channel fluorescent confocal microscopy experiments were carried out with HSP70 antibody and antibody to either microglia marker Iba-1 or astrocyte marker GFAP using P7 brain sections at 4 h of recovery after HI (Fig. 6). The brain sections at 4 h after HI in this animal model remain largely intact as shown in previous studies (Hu et al., 2000b; Liu et al., 2004). The confocal microscopy demonstrated that, in the P7 neocortical regions (Supplement Fig. 2s), HSP70 immunostaining (Fig. 6, upper panel, green color, arrows) overlapped with microglial marker Iba-1 (Fig. 6, upper panel, red color, arrows). However, HSP70 immunostaining (Fig. 6, lower panel, green color, arrows) did not overlap with astrocyte marker GFAP (Fig. 6, lower panel, red color, arrowheads). We did not perform the multi-channel fluorescent confocal microscopy experiments using P26 brain sections after HI with antibodies against HSP70 and either microglia marker Iba-1 or astrocyte marker GFAP. This is because the level of neuronal HSP70 induction is so pronounced that masks the weaker HSP70 immunostaining signal in microglial cells. However, it is highly likely that Hsp70 is also induced in microglia of mature brains after HI.

The basal constitutive levels of HSF1 and molecular chaperones

The development-dependent induction of molecular chaperones after HI could be owing to the different basal levels of constitutively expressed HSF1 and molecular chaperones. To study this, the basal levels of the master transcription factor HSF1, as well as heat shock cognate protein 70 (HSC70), HSP40, GRP78, GRP94, protein disulfide isomerase (PDI) and HSP60 were compared side-by-side between P7 and P26 brain samples on same Western blot membranes (Fig. 7). Samples were prepared from the sham-operated control brains

without HI. Beta-actin was used as a sample loading control (Fig. 7). The HSF1 level was significantly higher in P26 than P7 brain samples (Fig. 7). The levels of cytoplasmic residential chaperone HSC70 and HSP40 were virtually the same between P7 and P26 brain samples. However, the levels of residential ER molecular chaperones and folding enzyme GRP78, GRP94 and PDI were slightly but significantly lower in P26 compared to P7 brain samples (Fig. 7). The mitochondrial matrix HSP60 level was significantly higher in P26 than P7 brain samples (Fig. 7). The beta-actin level was basically the same between P7 and P26 brain tissue samples (Fig. 7, A and B).

DISCUSSION

This study shows that HI leads to nuclear translocation of HSF1, and induction of molecular chaperones in P26 mature neurons. In contrast, molecular chaperones are induced minimally in P7 immature neurons, but moderately in P7 microglia after HI, as shown in Figs. 1–6. Consistently, neonatal brain expresses a significantly lower level of HSF1, which may explain the minimal HSR in neonatal neurons after HI (see Fig. 7). Therefore, the effectiveness of therapeutic strategies targeting the stress pathway against HI may be significantly different between immature and mature brains. Furthermore, the induction of molecular chaperones occurs dramatically in the cytoplasm, and moderately in the ER lumen or mitochondrial matrix after HI (comparing Fig. 1 with Figs. 2 and 3). Regional and temporal distribution analyses further show that HSP70 protein is induced only slightly at 4 h, but more dramatically at 24 h when some HI-affected neurons are already dead after HI (see Fig. 1B). Therefore, the nature induction of molecular chaperones in mature brain may be somewhat late in protecting some HI dying neurons from acute HI injury.

The residential levels of molecular chaperones and folding enzyme

The low HSR in neonatal brain could be owing to higher residential molecular chaperones and folding enzymes. As shown in Fig. 7, this study shows that the basal levels of ER GRP78, GRP94 and PDI are slightly higher in sham control neonatal brain than those in mature brain. However, the basal level of cytosolic constitutive chaperones HSC70 and HSP40 are virtually the same, and the basal level of HSP60 was even lower in P7 than in P26 brain. Therefore, it is less likely that the differences in the stress responses between neonatal and mature brain after HI are owing to the preexisting levels of molecular chaperones.

The lack of HSR in P7 brain after HI may not be related to the cell injury levels

In this HI model, there is a gradient of HI or HI-induced cell injury densities, i.e., HI cell injury density is higher in the center core area, and lower in the surrounding area (because of the collateral circulation) in the same animals (see Fig. 2s). As shown in Fig. 1, there is very weak HSR throughout P7 brain sections after HI. Furthermore, the cell injury levels were controlled to be similar between P7 and P26 brains after HI in the animal model used in this study. Therefore, the lack of HSR in P7 brain after HI may not be related to the cell injury levels.

HSF1 is activated dramatically in mature neurons but minimally in neonatal neurons after HI

There is only limited information about HSF activation and nuclear translocation in neonatal or mature brains after HI. This study shows that neuronal nuclear translocation of HSF1 and expression of HSP70 occurs mainly in the mature brain after HI (see Figs. 4 and 5). A previous study shows that HSP70 protein is not induced in neurons after heat-shock in E18 primary neuronal cultures (Little et al., 1996; Hedtjärn et al., 2004). In a rat seizure model, hsp70 mRNA induction did not occur prior to P21 (Kalil et al., 1986). The levels of nuclear accumulation of HSF1 and induction of HSP70 are much higher in P40 than P2 rat brains after hyperthermia (Morrison et al., 2000). These previous studies are clearly in agreement with the results of the present study showing that HSF1 and HSP70 are altered more dramatically in P26, but slightly, if any, in P7 neurons after HI (see Figs. 1 and 5). These studies are also consistent with the fact that in the absence of cellular stress, HSF1 is sequestered to be inactive by HSP90 inhibitory protein complex. HI leads to HSF1 dissociation from the inhibitory complex and nuclear translocation for induction of cytoplasmic molecular chaperones mainly in mature neurons (Song et al., 2010; Islam et al., 2013).

This study shows that the level of HSF1 is significantly lower in P7 than P26 brain samples (see Fig. 7). It is known that the rate of the protein turnover is approximately three times higher in immature than that of the mature brain (Lajtha et al., 1979). Therefore, the lack of the cellular stress responses or HSR in P7 neonatal neurons after HI may be owing to the low level of HSF1 and the higher protein turnover capacity. Moreover, other mechanisms may also play a role in the lack of HSR in P7 neurons after HI. For instance, the higher HSP90 level in neonatal brain (see Fig. 7) may sequester more cellular HSF1, thus rendering the P7 neuronal stress response less sensitive to HI. Our previous studies show that induction of stress gene peaks at about 24 h, whereas neuronal death takes place at 48–72 h after brain ischemia in a rat transient forebrain ischemia model (Liu et al., 2005a; Truettner et al., 2009). Similarly, brain damage may further develop after 24 h following HI in the animal model used in the present study. Therefore, it remains to be studied whether induction of stress genes will further altered after 24 h in P7 brain after HI.

We noticed that, in P7 brain samples, the cytosolic HSF1 is decreased with a minimal increase in HSF1 in the nuclear P1 fraction, suggesting that P7 HSF1 may be degraded after HI (see Fig. 4A). The reason for that is unknown, but the following factors may contribute: (i) HSFs have at least two members HSF1 and HSF2 in neonatal neurons. HSF2 is constitutively active during neurodevelopment, rather than stress-related (Chang et al., 2006). The level of HSF1 is low at postnatal 5 day (P5) but reaches a plateau at P30, whereas the HSF2 level is just the opposite (Brown and Rush, 1999). HSF2 steers the formation of HSF1-HSF2 heterocomplexes and perturbs the binding to the heat shock elements (El Fatimy et al., 2014). As a result, HSF1-HSF2 dimers may be degraded in the cytosol; (ii) HSP70 is induced in non-neuronal cells such as microglia (as shown in Fig. 6). Therefore, the decrease in HSF1 may be in part due to its nuclear translocation followed by degradation in proliferating non-neuronal cells; and (iii) HSF1 transcriptional activity is tightly controlled through phosphorylation, sumoylation, and acetylation, which are

development-dependent events (Mohideen et al., 2009; Raychaudhuri et al., 2014) and may play a role in the HSF1 degradation after HI (Lee et al., 2008; Hu and Mivechi, 2011).

Cytosolic, ER and mitochondrial stress responses after HI

This study also shows that mRNAs of both Grp78 and Hsp60 are induced significantly but moderately only in P26 rats after HI as shown in Figs. 2A and 3A. However, the induction of Hsp60 and Grp78 mRNA-encoded **proteins** did not reach the statistical significance (see Figs. 2B and 3B). This may be due to the combination of: (i) the large constitutive HSP60 and GRP78 protein pools in sham control samples; and (ii) the induction degrees are less dramatic. Among molecular chaperones studied, cytoplasmic Hsp70 mRNA and HSP70 protein are induced strongest. A similar pattern of molecular chaperone induction is also seen in a global brain ischemia model (Truettner et al., 2009). Because induction of organelle-specific molecular chaperone reflects toxic protein aggregation in that particular organelle compartment, the more dramatic induction of cytoplasmic hsp70 mRNA may suggest that accumulation of misfolded proteins occurs more dramatically in the cytoplasm, but to a lesser degree in the ER lumen and mitochondrial matrix in P26 neurons after HI.

Significance of differential stress response between neonatal and mature neurons after HI

HI depletes ATP and disables ATP-dependent molecular chaperones for assisting nascent peptide chain folding, resulting in toxic aggregation of the protein translational complex in mature brain after ischemia (Hu et al., 2000a; Liu et al., 2005a; Zhang et al., 2006). Induction of molecular chaperones is an important defense mechanism for protecting neurons from toxic protein aggregation (Hu et al., 2000b; Liu et al., 2005b; Zhang et al., 2006; Badiola et al., 2011). Activation of HSF1 or HSR leads induction of more than 3000 genes encoding for classical molecular chaperones and non-classical cell protective proteins (Song et al., 2010; Islam et al., 2013). Therefore, activation of HSF1 may be a vital therapeutic strategy against ischemic brain injury. Previous studies have shown that increased expression of even a single molecular chaperone can offer neuroprotection in animal ischemia or ischemia-like cell culture models (Zhan et al., 2010; Kim et al., 2012; Stetler et al., 2012). Consistently, drug activation of HSF1 confers robust cell protection in cellular, worm, fly, and mouse or rat protein misfolding stress models including brain ischemia animal models (Lu et al., 2002; Harrison et al., 2008; Batulan et al., 2006; Neef et al., 2010; Liu et al., 2011; Verma et al., 2014; Ambade et al., 2014; Cha et al., 2014). This study shows that the levels of HSR and HSF1 activation are high in mature, but low in neonatal brain after HI. Therefore, drugs targeting HSR may be more effective against HI in mature than in neonatal brain.

This study further shows that relative to the induction of Hsp70 mRNA (see Fig. 1A), induction of HSP70 protein is delayed, i.e., slightly at 4 h, but dramatically at 24 h in P26 brain samples after HI as shown in Figs. 1B and 5B. This delayed induction may be because of the ribosomal protein synthesis machinery damage after brain ischemia, resulting in delayed translation of Hsp70 mRNA into protein, as shown in our previous studies (Liu et al., 2005a; Zhang et al., 2006). During this delayed period, some neurons have already died after HI (Hu et al., 2000b; Liu et al., 2004a). Therefore, this delayed induction of molecular chaperones may have less impact on these early HI dying neurons from acute HI injury, but

may help the remaining alive neurons to cope with protein misfolding stress after HI. Furthermore, induction of molecular chaperones may facilitate neuroplasticity during the recovery phase after HI. For instance, induction of stress proteins can improve learning process (Lin et al., 2004). Heat stress-induced preconditioning improves cognitive outcome after diffuse axonal injury in rats (Su et al., 2009). Therefore, a practical therapeutic strategy may be to activate HSF1 or to induce molecular chaperones before HI or at the early stage after HI to achieve a better neuroprotection.

Supplementary Material

Refer to Web version on PubMed Central for supplementary material.

Acknowledgments

Source of Funding

This work was supported by National Institutes of Health grants NS040407 and NS030291, AHA EIA grant 0940042N and Veteran Affair Merit Award I01BX001696-01.

References

Ambade A, Catalano D, Lim A, Kopoyan A, Shaffer SA, Mandrekar P. Pharmacological Inhibition of Heat Shock Protein 90 Alleviates Steatosis and Macrophage Activation in Murine Acute and Chronic Alcoholic Liver Injury. J Hepatol. 2014 [Epub ahead of print].

Badiola N, Penas C, Miñano-Molina A, Barneda-Zahonero B, Fadó R, Sánchez-Opazo G, Comella JX, Sabriá J, Zhu C, Blomgren K, Casas C, Rodríguez-Alvarez J. Induction of ER stress in response to oxygen-glucose deprivation of cortical cultures involves the activation of the PERK and IRE-1 pathways and of caspase-12. Cell Death Dis. 2011; 2:e149. [PubMed: 21525936]

Batulan Z, Taylor DM, Aarons RJ, Minotti S, Doroudchi MM, Nalbantoglu J, Durham HD. Induction of multiple heat shock proteins and neuroprotection in a primary culture model of familial amyotrophic lateral sclerosis. Neurobiol Dis. 2006; 24:213–225. [PubMed: 16950627]

Blomgren K, Leist M, Groc L. Pathological apoptosis in the developing brain. Apoptosis. 2007; 12:993–1010. [PubMed: 17453164]

Blumenfeld KS, Welsh FA, Harris VA, Pesenson MA. Regional expression of c-fos and heat shock protein-70 mRNA following hypoxia-ischemia in immature rat brain. J Cereb Blood Flow Metab. 1992; 12:987–995. [PubMed: 1400653]

Brown IR, Rush SJ. Cellular localization of the heat shock transcription factors HSF1 and HSF2 in the rat brain during postnatal development and following hyperthermia. Brain Res. 1999; 821:333–340. [PubMed: 10064819]

Cha JR, St Louis KJ, Tradewell ML, Gentil BJ, Minotti S, Jaffer ZM, Chen R, Rubenstein AE, Durham HD. A novel small molecule HSP90 inhibitor, NXD30001, differentially induces heat shock proteins in nervous tissue in culture and in vivo. Cell Stress Chaperones. 2014; 19:421–35. [PubMed: 24092395]

Chang Y, Ostling P, Akerfelt M, Trouillet D, Rallu M, Gitton Y, El Fatimy R, Fardeau V, Le Crom S, Morange M, Sistonen L, Mezger V. Role of heat-shock factor 2 in cerebral cortex formation and as a regulator of p35 expression. Genes Dev. 2006; 20:836–847. [PubMed: 16600913]

D'Souza SM, Brown IR. Constitutive expression of heat shock proteins Hsp90, Hsc70, Hsp70 and Hsp60 in neural and non-neural tissues of the rat during postnatal development. Cell Stress Chaperones. 1998; 3:188–99. [PubMed: 9764759]

El Fatimy R, Miozzo F, Le Mouël A, Abane R, Schwendimann L, Sabéran-Djoneidi D, de Thonel A, Massaoudi I, Paslaru L, Hashimoto-Torii K, Christians E, Rakic P, Gressens P, Mezger V. Heat shock factor 2 is a stress-responsive mediator of neuronal migration defects in models of fetal alcohol syndrome. EMBO Mol Med. 2014; 6:1043–1061. [PubMed: 25027850]

Fujimoto M, Nakai A. The heat shock factor family and adaptation to proteotoxic stress. FEBS J. 2010; 277:4112–4125. [PubMed: 20945528]

Fujimoto M, Nakai A. The heat shock factor family and adaptation to proteotoxic stress. FEBS J. 2010; 277:4112–25. [PubMed: 20945528]

Harrison EM, Sharpe E, Bellamy CO, McNally SJ, Devey L, Garden OJ, Ross JA, Wigmore SJ. Heat shock protein 90-binding agents protect renal cells from oxidative stress and reduce kidney ischemia-reperfusion injury. Am J Physiol Renal Physiol. 2008; 295:F397–405. [PubMed: 18562631]

Hartl FU, Hayer-Hartl M. Molecular chaperones in the cytosol: from nascent chain to folded protein. Science. 2002; 295:1852–1858. [PubMed: 11884745]

Hedtjärn M, Mallard C, Eklind S, Gustafson-Brywe K, Hagberg H. Global gene expression in the immature brain after hypoxia-ischemia. J Cereb Blood Flow Metab. 2004; 24:1317–1332. [PubMed: 15625407]

Hu BR, Janelidze S, Ginsberg MD, Busto R, Liu CL. Protein aggregation after focal brain ischemia and reperfusion. J Cereb Blood Flow Metab. 2001; 21:865–875. [PubMed: 11435799]

Hu BR, Liu CL, Ouyang Y, Blomgren K, Siesjö BK. Involvement of caspase-3 in cell death after hypoxia-ischemia declines during brain maturation. J Cereb Blood Flow Metab 2000. 2000b; 20:1294–1300.

Hu BR, Martone ME, Jones YZ, Liu CL. Protein aggregation after transient cerebral ischemia. J Neurosci. 2000a; 20:3191–3199. [PubMed: 10777783]

Hu BR, Park M, Martone ME, Fischer WH, Ellisman MH, Zivin JA. Assembly of proteins to postsynaptic densities after transient cerebral ischemia. J Neurosci. 1998; 18:625–633. [PubMed: 9425004]

Hu Y, Mivechi NF. Promotion of heat shock factor Hsf1 degradation via adaptor protein filamin A-interacting protein 1-like (FILIP-1L). J Biol Chem. 2001; 286:31397–31408. [PubMed: 21784850]

Islam A, Deuster PA, Devaney JM, Ghimbovschi S, Chen Y. An exploration of heat tolerance in mice utilizing mRNA and microRNA expression analysis. PLoS One. 2013; 8:e72258. [PubMed: 23967293]

Kalil K, Skene JH. Elevated synthesis of an axonally transported protein correlates with axon outgrowth in normal and injured pyramidal tracts. J Neurosci. 1986; 6:2563–2570. [PubMed: 3746423]

Kim N, Kim JY, Yenari MA. Anti-inflammatory properties and pharmacological induction of Hsp70 after brain injury. Inflammopharmacology. 2012; 20:177–85. [PubMed: 22246599]

Lajtha A, Dunlop D, Patlak C, Toth J. Compartments of protein metabolism in the developing brain. Biochim Biophys Acta. 1979; 561:491–501. [PubMed: 427169]

Lee YJ, Kim EH, Lee JS, Jeoung D, Bae S, Kwon SH, Lee YS. HSF1 as a mitotic regulator: phosphorylation of HSF1 by Plk1 is essential for mitotic progression. Cancer Res. 2008; 68:7550–7560. [PubMed: 18794143]

Lin YW, Yang HW, Min MY, Chiu TH. Heat-shock pretreatment prevents suppression of long-term potentiation induced by scopolamine in rat hippocampal CA1 synapses. Brain Res. 2004; 999:222–226. [PubMed: 14759502]

Little E, Tocco G, Baudry M, Lee AS, Schreiber SS. Induction of glucose-regulated protein (glucose-regulated protein 78/BiP and glucose-regulated protein 94) and heat shock protein 70 transcripts in the immature rat brain following status epilepticus. Neuroscience. 1996; 75:209–219. [PubMed: 8923535]

Liu AY, Mathur R, Mei N, Langhammer CG, Babiarz B, Firestein BL. Neuroprotective drug riluzole amplifies the heat shock factor 1 (HSF1)- and glutamate transporter 1 (GLT1)-dependent cytoprotective mechanisms for neuronal survival. J Biol Chem. 2011; 286:2785–94. [PubMed: 21098017]

Liu AY, Mathur R, Mei N, Langhammer CG, Babiarz B, Firestein BL. Neuroprotective drug riluzole amplifies the heat shock factor 1 (HSF1)- and glutamate transporter 1 (GLT1)-dependent cytoprotective mechanisms for neuronal survival. J Biol Chem. 2011; 286:2785–94. [PubMed: 21098017]

Liu C, Chen S, Kamme F, Hu BR. Ischemic preconditioning prevents protein aggregation after transient cerebral ischemia. Neuroscience. 2005b; 134:69–80. [PubMed: 15939539]

Liu CL, Ge P, Zhang F, Hu BR. Co-translational protein aggregation after transient cerebral ischemia. Neuroscience. 2005a; 134:1273–84. [PubMed: 16039801]

Liu CL, Siesjö BK, Hu BR. Pathogenesis of hippocampal neuronal death after hypoxia-ischemia changes during brain development. Neuroscience. 2004; 127:113–123. [PubMed: 15219674]

Lu A, Ran R, Parmentier-Batteur S, Nee A, Sharp FR. Geldanamycin induces heat shock proteins in brain and protects against focal cerebral ischemia. J Neurochem. 81:355–364. [PubMed: 12064483]

Martin LJ, Furuta A, Blackstone CD. AMPA receptor protein in developing rat brain: glutamate receptor-1 expression and localization change at regional, cellular, and subcellular levels with maturation. Neuroscience. 1998; 83:917–928. [PubMed: 9483574]

Mohideen F, Capili AD, Bilimoria PM, Yamada T, Bonni A, Lima CD. A molecular basis for phosphorylation-dependent SUMO conjugation by the E2 UBC9. Nat Struct Mol Biol. 2009; 16:945–952. [PubMed: 19684601]

Morrison AJ, Rush SJ, Brown IR. Heat shock transcription factors and the hsp70 induction response in brain and kidney of the hyperthermic rat during postnatal development. J Neurochem. 2000; 75:363–372. [PubMed: 10854282]

Neef DW, Jaeger AM, Thiele DJ. Heat shock transcription factor 1 as a therapeutic target in neurodegenerative diseases. Nat Rev Drug Discov. 2011; 10:930–944. [PubMed: 22129991]

Ponten U, Ratcheson RA, Salford L, Siesjö BK. Optimal freezing conditions for cerebral metabolites in rats. J Neurochem. 1973; 21:1127–1138. [PubMed: 4761701]

Raychaudhuri S, Loew C, Körner R, Pinkert S, Theis M, Hayer-Hartl M, Buchholz F, Hartl FU. Interplay of acetyltransferase EP300 and the proteasome system in regulating heat shock transcription factor 1. Cell. 2014; 156:975–785. [PubMed: 24581496]

Rice JE 3rd, Vannucci RC, Brierley JB. The influence of immaturity on hypoxic-ischemic brain damage in the rat. Ann Neurol. 1981; 9:131–141. [PubMed: 7235629]

Romijn HJ, Hofman MA, Gramsbergen A. At what age is the developing cerebral cortex of the rat comparable to that of the full-term newborn human baby? Early Hum Dev. 1991; 26:61–67. [PubMed: 1914989]

Sarge KD, Park-Sarge OK, Kirby JD, Mayo KE, Morimoto RI. Expression of heat shock factor 2 in mouse testis: potential role as a regulator of heat-shock protein gene expression during spermatogenesis. Biol Reprod. 1994; 50:1334–1343. [PubMed: 8080921]

Song S, Kole S, Precht P, Pazin MJ, Bernier M. Activation of heat shock factor 1 plays a role in pyrrolidine dithiocarbamate-mediated expression of the co-chaperone BAG3. Int J Biochem Cell Biol. 2010; 42:1856–1863. [PubMed: 20692357]

Stetler RA, Gao Y, Zhang L, Weng Z, Zhang F, Hu X, Wang S, Vosler P, Cao G, Sun D, Graham SH, Chen J. Phosphorylation of HSP27 by protein kinase D is essential for mediating neuroprotection against ischemic neuronal injury. J Neurosci. 2012; 32:2667–82. [PubMed: 22357851]

Su Z, Han D, Sun B, Qiu J, Li Y, Li M, Zhang T, Yang Z. Heat stress preconditioning improves cognitive outcome after diffuse axonal injury in rats. J Neurotrauma. 2009; 26:1695–1706. [PubMed: 19785543]

Tang K, Liu C, Kuluz J, Hu B. Alterations of CaMKII after hypoxia-ischemia during brain development. J Neurochem. 2004; 912:429–437. [PubMed: 15447676]

Towfighi J, Mauger D, Vannucci RC, Vannucci SJ. Influence of age on the cerebral lesions in an immature rat model of cerebral hypoxia-ischemia: a light microscopic study. Brain Res Dev Brain Res. 1997; 100:149–160. [PubMed: 9205806]

Towfighi J, Mauger D. Temporal evolution of neuronal changes in cerebral hypoxia-ischemia in developing rats: a quantitative light microscopic study. Brain Res Dev Brain Res. 1998; 109:169–177. [PubMed: 9729365]

Truettner JS, Hu K, Liu CL, Dietrich WD, Hu B. Subcellular stress response and induction of molecular chaperones and folding proteins after transient global ischemia in rats. Brain Res. 2009; 1249:9–18. [PubMed: 18996359]

Vannucci RC, Vannucci SJ. A model of perinatal hypoxic-ischemic brain damage. Ann N Y Acad Sci. 1997; 835:234–49. [PubMed: 9616778]

Verma P, Pfister JA, Mallick S, D'Mello SR. HSF1 protects neurons through a novel trimerization- and HSP-independent mechanism. J Neurosci. 2014; 34:1599–1612. [PubMed: 24478344]

Vydra N, Toma A, Glowala-Kosinska M, Gogler-Piglowska A, Widlak W. Overexpression of Heat Shock Transcription Factor 1 enhances the resistance of melanoma cells to doxorubicin and paclitaxel. BMC Cancer. 2013; 13:504. [PubMed: 24165036]

Wang X, Carlsson Y, Basso E, Zhu C, Rousset CI, Hagberg H, et al. Developmental shift of cyclophilin D contribution to hypoxic-ischemic brain injury. J Neurosci. 2009; 29:2588–2596. [PubMed: 19244535]

Wu C. Heat shock transcription factors : structure and regulation. Annu Rev Cell Dev Biol. 1995; 11:441–469. [PubMed: 8689565]

Xu YM, Huang DY, Chiu JF, Lau AT. Post-translational modification of human heat shock factors and their functions: a recent update by proteomic approach. J Proteome Res. 2012; 11:2625–2634. [PubMed: 22494029]

Zhan X, Ander BP, Liao IH, Hansen JE, Kim C, Clements D, Weisbart RH, Nishimura RN, Sharp FR. Recombinant Fv-Hsp70 protein mediates neuroprotection after focal cerebral ischemia in rats. Stroke. 2010; 41:538–543. [PubMed: 20075343]

Zhang F, Liu CL, Hu BR. Irreversible aggregation of protein synthesis machinery after focal brain ischemia. J Neurochem. 2006; 98:102–112. [PubMed: 16805800]

Zhu C, Qiu L, Wang X, Xu F, Nilsson M, Blomgren K, et al. Age-dependent regenerative responses in the striatum and cortex after hypoxia-ischemia. J Cereb Blood Flow Metab. 2009; 29:342–354. [PubMed: 18985054]

Highlights

- This paper studied the stress response after brain hypoxia-ischemia (HI) in rat.
- HSF1 and stress proteins were analyzed Western blotting and confocal microscopy
- Expression of stress gene mRNAs was analyzed by in situ hybridization
- The results show that the stress response after HI is development-dependent.
- The stress response is pronounced in mature, but negligible in neonatal neurons.

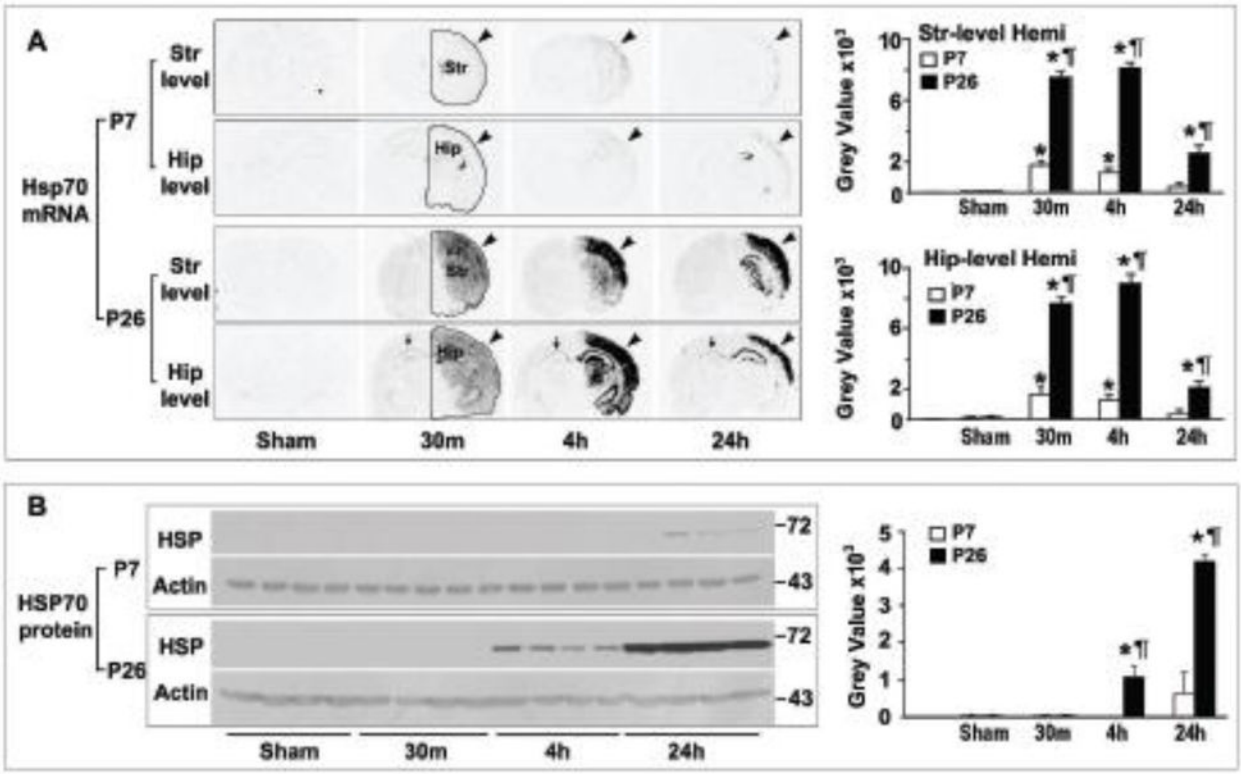

Fig. 1.

Expression of HSP70 after HI. Brain sections or tissue samples were from P7 or P26 sham-operated control rats and rats subjected to HI followed by 0.5, 4 and 24 h of recovery. ***A-left panels:*** Autoradiographs of *in situ* hybridization of hsp70 mRNA. Arrowheads point to the HI ipsilateral hemispheres. Arrows indicate the P26 contralateral CA1 area. The drawing areas indicate the ipsilateral hemisphere; ***A-right panels:*** Quantitative analysis of the hsp70 mRNA levels in the entire striatal level HI hemisphere (upper, Str-level Hemi) and the entire hippocampal level HI hemisphere (lower, Hip-level Hemi) of P7 (open bar) and P26 (black bar) brain sections, as delineated in the 30 min brain sections of Fig. 1A-left panels. ***B-left panels:*** Western blotting of HSP70 protein and beta-actin in tissue homogenates. Molecular size in kDa is indicated on the right; ***B-right panels:*** Quantitative analysis of the HSP70 protein level in P7 (open bar) and P26 (black bar) brain tissue samples. The HSP70 data were normalized with beta-actin loading control. The grey density value data are mean ± standard error (SEM) (n = 4). One-way ANOVA followed by Tukey's post-hoc test. *denotes $p<0.01$ between sham-operated control and post-HI animals. ¶ indicates $p<0.01$ between P7 and P26 groups.

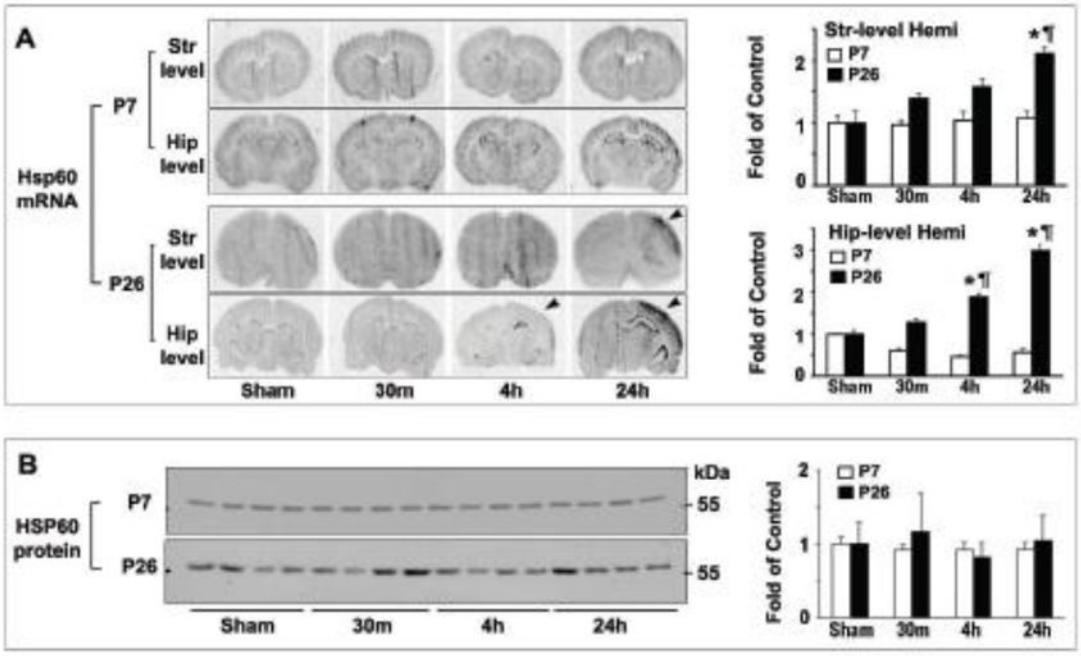

Fig. 2.

Expression of HSP60 after HI. Brain sections or tissue samples were obtained from the same sets of brains as in figure 1. ***A-left panels:*** Autoradiographs of *in situ* hybridization of hsp60 mRNA; ***A-right panels:*** Quantitative analysis of the hsp60 mRNA levels in the entire striatal level HI hemisphere (upper, Str-level Hemi) and the entire hippocampal level HI hemisphere (lower, Hip-level Hemi) of P7 (open bar) and P26 (black bar) brain sections, as delineated in the 30 min brain sections of Fig. 1A-left panels. ***B-left panels:*** Western blotting of HSP60 protein. Molecular size marker in kDa is indicated on the right; ***B-right panels:*** Quantitative analysis of the HSP60 protein level in P7 (open bar) and P26 (black bar) brain samples. The HSP60 data were normalized with beta-actin loading control. Data are mean ± standard error (SEM) (n = 4) and expressed as fold of control. One-way ANOVA followed by Tukey's post-hoc test. *denotes $p<0.01$ between sham-operated control and post-HI animals. ¶ indicates $p<0.01$ between P7 and P26 groups.

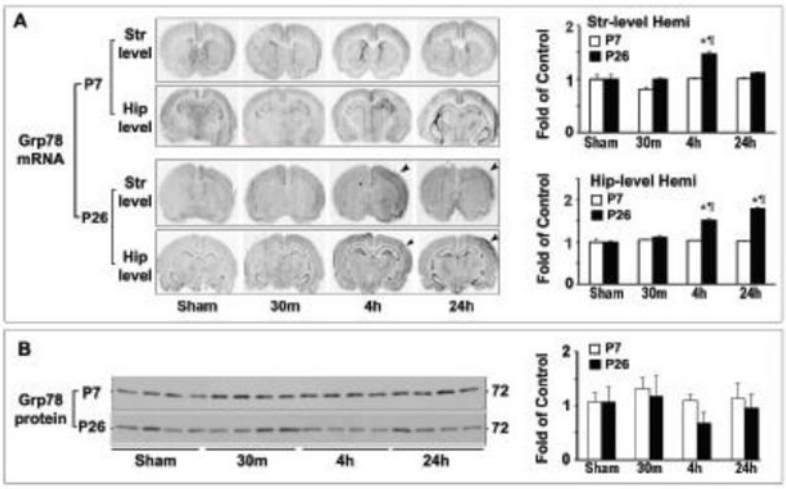

Fig. 3.

Expression of grp78 after HI. The brain sections or tissue samples were obtained from the same sets of brains of figure 1. ***A-left panels:*** Autoradiographs of *in situ* hybridization of grp78 mRNA; ***A-right panels:*** Quantitative analysis of the grp78 mRNA levels in the entire striatal level HI hemisphere (upper, Str-level Hemi) and the entire hippocampal level HI hemisphere (lower, Hip-level Hemi) of P7 (open bar) and P26 (black bar) brain sections, as delineated in the 30 min brain sections of Fig. 1A-left panels. ***B-left panels:*** Western blotting of GRP78 protein. Molecular size marker in kDa is indicated on the right; ***B-right panels:*** Quantitative analysis of the GRP78 protein level in P7 (open bar) and P26 (black bar) brain tissue samples. The GRP78 data were normalized with beta-actin loading control. Data are mean ± standard error (SEM) (n = 4) and expressed as fold of control. *denotes $p<0.01$ between sham-operated control and post-HI animals. ¶ indicates $p<0.01$ between P7 and P26 groups. One-way ANOVA followed by Tukey's post-hoc test.

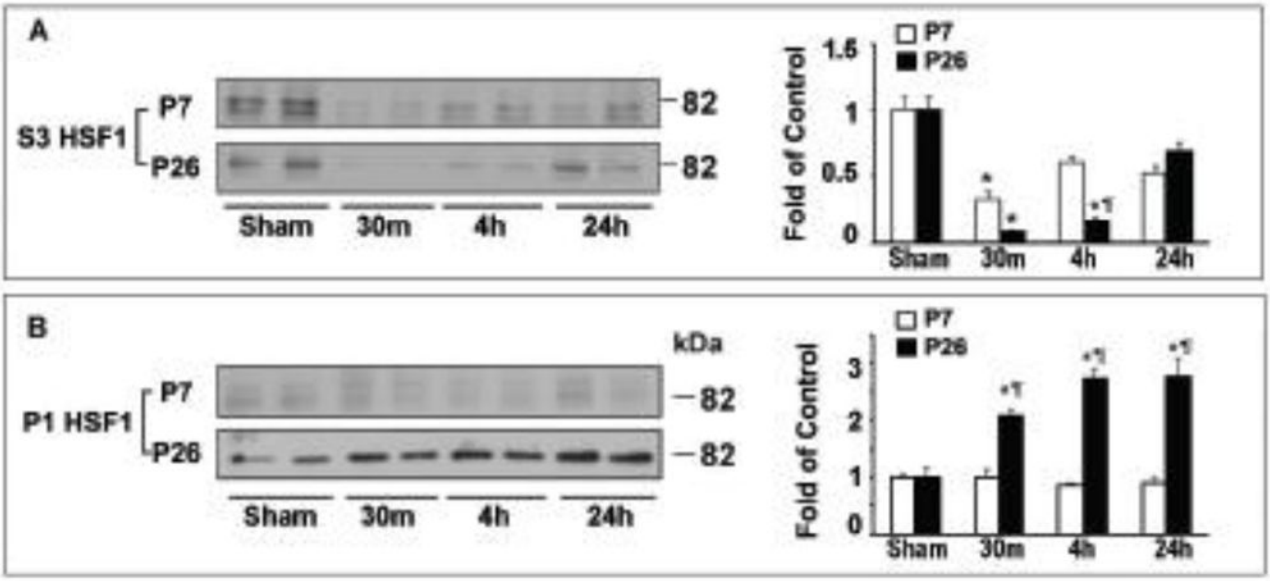

Fig. 4.

(A) Immunoblotting of HSF1 in S3 ***(upper panels)*** and P1 ***(lower panels)*** fractions after HI. Tissue samples were prepared from the same brains of figure 1. ***(B)*** Quantitative analysis of the HSF1 levels in in S3 ***(upper panel)*** and P1 ***(lower panel)*** fractions prepared from P7 (open bar) and P26 (black bar) brain samples. The HSF1 data were normalized with beta-actin loading control. Data are mean ± standard error (SEM) (n = 4) and expressed as fold of control. One-way ANOVA followed by Tukey's post-hoc test. *denotes $p<0.01$ between sham-operated control and post-HI animals. ¶ indicates $p<0.01$ between P7 and P26 groups.

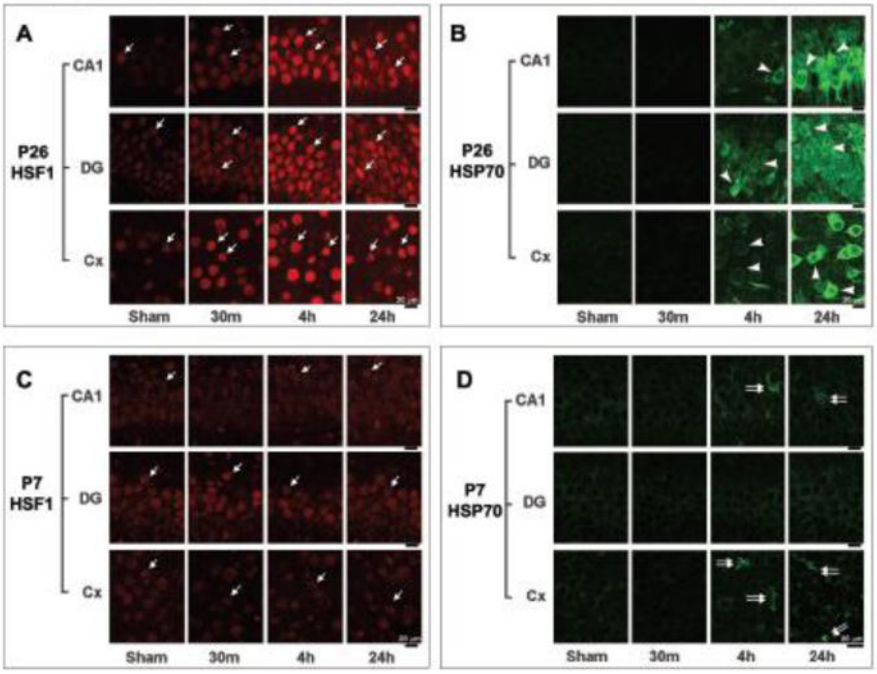

Fig. 5.

Double immunostaining confocal microscopy of HSF1 (left panels, red) and HSP70 (right panels, green) of P26 brain sections ***(A and B)*** and of P7 brain sections ***(C and D)***. Brain sections were from sham-operated control rats and rats subjected to HI followed by 0.5, 4 and 24 h of recovery. Three brain sections from three different rats in each experimental group were used in these confocal microscopic analyses. The results were reproducible. Arrows point to neuronal nuclei (**A** and **C**); Arrowheads indicate neuronal HSP70 immunostaining ***(B)***; Double-arrows point to non-neuronal HSP70 immunostaining ***(D)***. Scale bar = 20 μm.

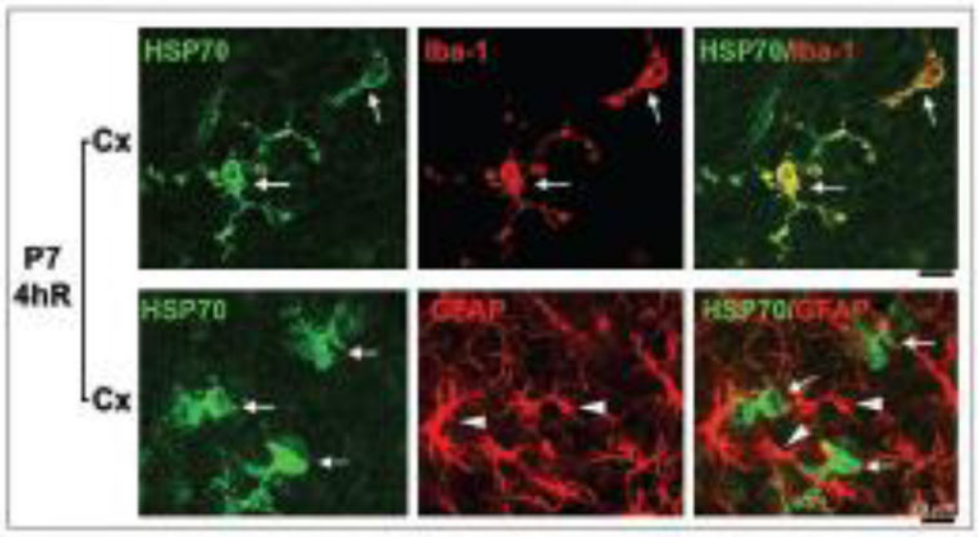

Fig. 6.

Double immunostaining confocal microscopy of HSP70 and Iba-1 or GFAP in P7 brain sections after HI. Brain sections were from P7 rats subjected to HI followed by 4 h of recovery (P7 4hR). ***Upper:*** HSP70 immunostaining (left, green) and microglia marker Iba-1 immunostaining (middle, red) are overlapped each other (right). Arrows point to immunopositive microglia. ***Lower:*** HSP70 immunostaining (left, green) and astrocyte marker GFAP immunostaining (middle, red) are not overlapped each other (right). Arrows point to immunopositive microglia. Arrowheads indicate astrocytes. Scale bar = 20 μm.

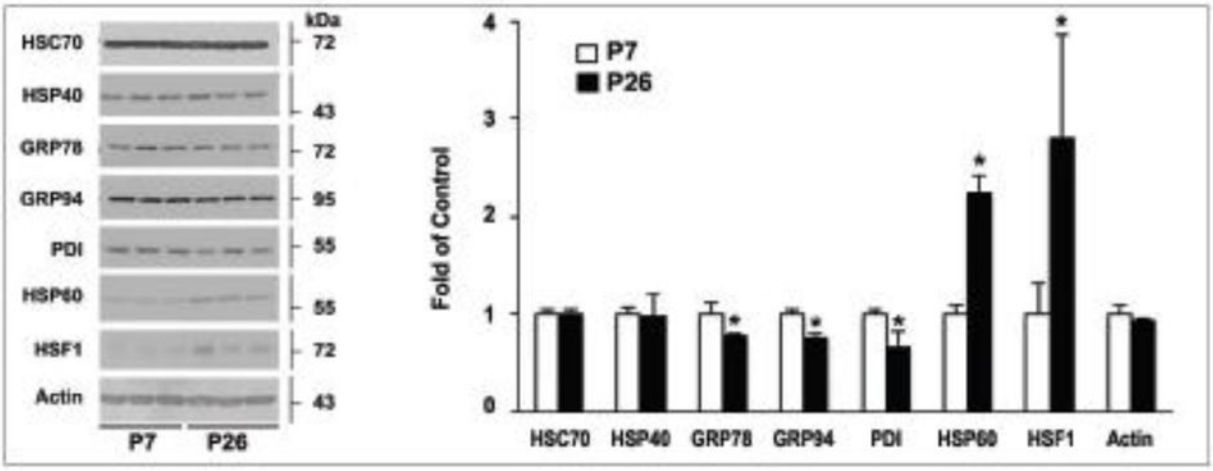

Fig. 7.

(A) Immunoblotting of HSC70, HSP40, GRP78, GRP94, PDI, HSP60, HSF1, and beta-actin. The brain tissue samples were prepared from P7 and P27 non-ischemic control rats. ***(B)*** Quantitative analysis of HSC70, HSP40, GRP78, GRP94, PDI, HSP60, HSF1 and beta-actin bands. Data are mean ± standard error (SEM) (n = 3) and expressed as fold of control. **p*< 0.01 between P7 and P26 samples, unpaired t-test.